PAPER

Toluene adsorption and capacity regeneration using zeolite-based monolith and activated carbon fiber felt

Melanie Moses-DeBusk, [ID] * Mengjia Tang, [ID] Kai Li, [ID] Keju An, [ID] William P. Partridge [ID] and Kashif Nawaz [ID]

Common adsorbents studied to remove volatile organic compounds (VOCs) from indoor air can release previously adsorbed VOCs back into the indoor space when the adsorbent is saturated or if the VOC concentration fluctuates. A durable adsorbent with a continuous regeneration strategy could prevent this recontamination of the indoor air and reduce adsorbent disposal waste. A deeper understanding of the adsorption and desorption behavior of VOC adsorbents is needed to create an efficient regeneration strategy. This study investigated the adsorption and thermal desorption behavior of toluene on two different adsorbents, (1) a zeolite-based adsorbent and (2) an activated carbon fiber (ACF) felt. Consistent adsorption behavior across a series of toluene concentrations was used to experimentally determine effective adsorption capacity. When the cumulative adsorption between thermal regeneration steps was maintained below the maximum effective capacity with 0% breakthrough, the zeolite-based adsorbent was found to effectively minimize passive desorption. The impact of regeneration feed conditions, such as inert, oxidizing, humidified air, on thermal desorption was examined. These conditions influenced desorption of the zeolite-based adsorbent but had minimal impact on the ACF felt adsorbent, which would lead to different regeneration schedules and methods for applications in buildings' heating, ventilation, and air conditioning (HVAC) systems.

Environmental significance

The use of adsorbents for removal of volatile organic compounds (VOCs) from indoor air should prevent passive desorption back into indoor space when concentrations drop or are low. Integration of the adsorbent into the building ventilation system would be further improved if in-line regeneration of the adsorbent under mild conditions is possible. An understanding of adsorption capacity and desorption conditions are needed to design effective integration. To assist in this design related to the potential adsorbent placement locations in the intake or recirculated air flow and how often the adsorbent may need to be bypassed for regeneration, this paper investigates the maximum adsorption without passive desorption and the environmental conditions required for regeneration for two different types of adsorbents.

1. Introduction

The built environment, especially with regard to indoor air quality (IAQ), plays a vital role in maintaining and promoting the well-being of humans.[1] As a result of spending approximately 87% of the time inside buildings,[2] people have a high exposure to indoor air contaminants. Indoor exposure to volatile organic compounds (VOCs) is of particular concern because VOCs tend to be significantly more abundant in buildings compared to outdoors due to emissions from building materials and furnishings (*e.g.*, pressed wood products and carpets), occupants (*e.g.*, breath, skin, and personal care products), and their activities (*e.g.*, cooking and cleaning).[3] Continuous

monitoring of VOC concentrations inside and outside of a residential house for one week showed that the indoor concentrations were significantly higher than outdoors, with an indoor/outdoor ratio of 20 for formaldehyde.[4] A field study of 37 elementary and K-8 schools demonstrated an indoor/outdoor ratio between unity and ten for most VOCs.[5] Several VOCs commonly found inside buildings are carcinogenic, such as formaldehyde, benzene, and acetaldehyde, or sensory irritants, such as acrolein; moreover these VOCs have been reported as above safe levels set by the U.S. Environmental Protection Agency (EPA) or California Office of Environmental Health Hazard Assessment (OEHHA) in a large percentage of residences in the U.S. or countries with similar lifestyles according to 77 prior studies.[6] Of 37 small- and medium-sized commercial buildings in California, over 80% exceeded OEHHA's chronic Reference Exposure Level (REL) of formaldehyde and over 50%

Buildings and Transportation Science Division, Oak Ridge National Laboratory, Oak Ridge, TN 37830, USA. E-mail: mosesmj@ornl.gov

exceed U.S. EPA's Reference Concentration (RfC) for chronic inhalation exposure of acetaldehyde.[7] As building enclosures become tighter to reduce infiltration and save energy, indoor VOC concentrations are likely to rise. Therefore, reducing indoor VOC exposure has become an urgent need for public health.

Applying air cleaning devices in building heating, ventilation, and air conditioning (HVAC) systems can be an effective and energy efficient approach to control VOCs by reducing the need for outdoor air ventilation.[8] As allowed by the IAQ Procedure in ASHRAE Standard 62.1 "Ventilation and Acceptable Indoor Air Quality", the outdoor air intake rate can be determined by meeting the concentration limits of design compounds that contain 11 VOCs in replacement of a prescriptive rate based on space and occupancy.[9] To efficiently and effectively improve indoor air quality without energy wasting due to outdoor-air exchange, identifying and optimizing VOC removal technologies that are ready for application in buildings is critical.

VOC abatement methods can be divided into two categories – recovery and conversion/destruction – depending on whether VOCs are trapped or converted into different compounds, respectively.[10] Adsorption is a highly promising trapping method, known for its relatively low cost and proven effectiveness in achieving high removal rates and fewer byproducts compared to destruction methods such as photocatalytic oxidation and plasma catalysis.[10,11] The most popular materials for VOC adsorption are activated carbon and zeolites.[12] Filters containing pure granular activated carbon (GAC) have been reported to maintain over 90% efficiency when challenged by 4 ppm toluene for 30 h.[13] Packed bed reactor evaluation of toluene removal by GAC have shown adsorption capacities ranging from 350 to 600 mg g^{-1} depending on the bed depth, challenge concentration, and flow rate.[14] Compared to GAC, activated carbon fiber (ACF) that can be made into cloth or felt has a higher adsorption efficiency and is easier to regenerate.[15,16] When tested under identical conditions using the same weight of the adsorbent for removing toluene, the breakthrough time for ACF (45 min) was nearly two times longer than GAC (25 min). Zeolites are another adsorbent suitable for VOCs due to their high surface area, pore volume, and thermal stability.[17] One study demonstrated toluene adsorption capacities ranging from 80 to 210 mg g^{-1} for different types of zeolites.[18] The referenced absolute GAC, ACF and zeolite capacities are not directly comparable due to differences between the referenced works. Nevertheless, these ACF and zeolite adsorption capacities suggest them to be good candidates for cleaning VOCs from indoor air.

Several regeneration methods have been applied to ACF and zeolite adsorbents to facilitate continuous use. Following toluene saturation of ACF cloth, electrothermal heating for 30 min at 145 °C was found to recover 75% adsorption capacity in the first adsorption–desorption cycle but no further loss in capacity occurred over the following four cycles.[19] Another study used ACF cloth to adsorb and desorb a mixture of VOCs below 50 ppb in a cyclic process and reported greater than 60% toluene removal efficiency was maintained over five, 12 h adsorption – 15 min, 150 °C regeneration cycles. Circulating a DC current through the ACF cloth was used in this study to heat the ACF cloth to 150 °C during the 15 min regenerations.[8] A similar study reported passing a DC current through a ACF cloth for 60 min to investigate desorption temperature impacts and found that 150 °C led to more complete desorption of toluene compared to 75 °C and 100 °C, while increasing the temperature higher to 200 °C did not provide any further improvement.[15] A study on regeneration of zeolite adsorbents found that more toluene was desorbed by microwave heating at 500 W for 10 min (the final temperature of the adsorbents varied from 60 to 184 °C depending on the type of the zeolite adsorbent and gas stream) than conventional heating to 300 °C at a heating rate of 5 °C min^{-1} using an electric furnace.[17] A recent study demonstrated that a 85% toluene adsorption capacity could be recovered over five adsorption–desorption cycles on zeolites by increasing temperature from 25 °C to 180 °C during desorption.[18]

The main challenges to real-world application of ACF and zeolites to improve indoor air quality are degrading adsorption efficiency over time and passive or uncontrolled VOC desorption. While ACFs and zeolites have high toluene adsorption capacities, that capacity fills via an "S" shaped breakthrough curve;[15,18] efficient initial adsorption by highly active and/or accessible adsorption sites, followed by progressively degraded adsorption due to fewer active and/or accessible sites. The high adsorption capacity but slow rate of adsorption, in some applications, may require that the adsorbent be replaced before the maximum adsorption is reached to prevent the concentration downstream of the adsorbents from increasing to undesirable levels in the breathing zone of building occupants. Additionally, the adsorbent itself could become a VOC source if it allows passive VOC desorption when exposed to airflows with relatively low VOC concentrations. It was found that 40.9% of toluene previously adsorbed on GAC was passively desorbed when exposed to Helium for 2 h.[20] This reversibility of adsorption in the presence of concentration dynamics was recently reported for benzene on GAC and occurred even when the GAC was far from saturation.[21] The combined issue of slow adsorption rates and passive desorption may be addressed by regenerating the adsorbents on-site on a regular basis to both effectively clean air and reduce waste caused by using non-reusable adsorbents. For optimal VOC removal system, it is important to determine the regeneration frequency and conditions and to quantify the fractional or effective capacities that can be recovered.

While literature exists describing the adsorption–desorption behavior and regeneration of adsorbents for VOC removal, the information on relating the breakthrough and adsorption capacity at high contaminant concentrations to lower ones and the effectiveness of adsorbent regeneration under varying conditions is still lacking. A systematic bench scale experimental study is needed especially for zeolites and activated carbon fibers that are highly promising for IAQ applications in buildings. The objectives of this study were to understand the performance of two distinctly different adsorbents – a zeolite-based adsorbent and an activated carbon fiber felt – in removing toluene and being regenerated for reuse if

© 2026 The Author(s). Published by the Royal Society of Chemistry

Environ. Sci.: Adv., 2026, **5**, 450–462 | **451**

incorporated into HVAC systems. The temperature and oxidative environment impact on the regeneration process of both adsorbents along with adsorption capacity by considering passive desorption were investigated to enable the in-line regeneration at an optimal frequency, temperature and environment. Toluene was used as the VOC in this study because of its similar structure to other more hazardous aromatic hydrocarbons and has been widely used to represent VOCs in literature on the adsorption and desorption behavior of adsorbents.[22–25] The toluene adsorption on the two adsorbents was studied under three challenge concentrations (60, 140, and 200 ppm) to establish the relationship between the breakthrough time and total mass challenged and determine the effective adsorption capacity of each adsorbent. The impacts of temperature (30 °C to 300 °C) and gas compositions (inert *vs.* oxidizing and dry *vs.* humidified) during regeneration were investigated to aid in future development of efficient regeneration strategies.

2. Methodology

2.1. Adsorbent materials

The two adsorbent materials that were evaluated, *i.e.*, zeolite-based monolith and activated carbon felt (ACF-1600), are shown in Fig. 1.

2.1.1. Zeolite-based washcoat. The zeolite-based washcoated adsorbent, designed for hydrocarbon trapping in light-duty engine exhaust during vehicle cold-starts, was provided by Umicore. A 2 L (5.66 inch OD × 4.84 inch long) channel flow monolith washcoated with the catalyzed zeolite had 400 channels per square inch (cpsi) with 4 mil (0.004 in) thick channel walls. Common washcoating practice uses a mass density, p_{wc_m}, on the monolith of approximately of 2 g in^{-3} (0.122 mg mm^{-3}).

The 2 L washcoated monolith was degreened by SGS North America Inc. at 700 °C for 50 h using stationary engine exhaust under the recommended US Drive protocol.[26] The low-temperature hydrocarbon trapping target of this zeolite-based monolith made it a compelling material to investigate as a VOC adsorbent for IAQ applications. Smaller monolith samples were cut from the front of the 2 L zeolite monolith for evaluation. The Fig. 1(A) schematic describes the

macrostructure of a typical washcoated monolith. For all samples studied, the length and number of washcoated channels in the sample were used to calculate a relative volume of monolith for sample-to-sample comparisons. Adsorption results were normalized to the estimated mass of the zeolite-based adsorbent (M_{ZB}). The washcoated adsorbent was calculated from the number (N_{ch}) and length (L_{ch}) of monolith channels used and the number of channels per cross-sectional area of the 400 cpsi monolith (A_{ch}, 0.620 ch mm^{-2}) according to eqn (1).

$$M_{ZB} = \frac{p_{wc_m} \times N_{ch} \times L_{ch}}{A_{ch}} \tag{1}$$

2.1.2. ACF-1600. The activated carbon felt (ACF-1600, Fig. 1(B)) was purchased from CeraMaterials. The ACF-1600 felt had a specific surface area of 1500 m^2 g^{-1} and micropore volume of 0.8–1.2 mL g^{-1}. While some literature studies have used ACF cloth which contains woven ACF, this study used an ACF felt which has non-woven fibers to reduce the potential for the increased backpressure that woven cloth fibers can cause. Results were normalized by the measured ACF-sample weight (M_{ACF}).

2.2. Maximum adsorption capacity measurements

A dynamic vapor sorption (DVS) system (DVS Resolution, Surface Measurement Systems Ltd) was used to measure the toluene adsorption isotherm and capacity of the adsorbent materials in a dry air environment. Before measurements, the adsorbent samples were dried at 80 °C in an oven overnight to remove moisture and any adsorbed gases. Then the dried sample of ACF-1600 or zeolite-based adsorbent was loaded on the stainless-steel pan in the DVS adsorption chamber. Samples used for these DVS studies were small rectangular pieces of the ACF felt (17–20 mg; 25.5–30 mm^2) and 30 channels (13.35 mm long; 0.0788 g washcoat) of the zeolite-based adsorbent washcoated monolith. The toluene partial pressure (P/P_0) was increased from 0 to 90% in 10% steps. All measurements were performed at ~30 °C using a built-in bubbler system with dry air carrier gas to introduce gaseous toluene. The adsorption isotherms were derived for each adsorbent from sample weight measured by the DVS' microbalance after each toluene adsorption step (M_{DVS}) normalized by the neat adsorbent sample mass (M_{adsorb}).Where the maximum adsorption capacity ($\Delta m_{cap,max}$) refers to the greatest toluene adsorption measured during the dry partial pressure sweep, according to eqn (2).

$$\Delta m_{cap} = \frac{M_{DVS} - M_{adsorb}}{M_{adsorb}} \tag{2}$$

2.3. Adsorption and desorption measurements

Fig. 2 shows the custom bench scale gas reactor capable of generating doped humidified air flows that were used for toluene adsorption and desorption experiments. Synthetic air flow (20% O$_2$, 400 ppm CO$_2$, N$_2$ balance) was produced using mass flow controllers to meter gas standards from compressed cylinders. The MKS mass flow controllers used meter gas flow
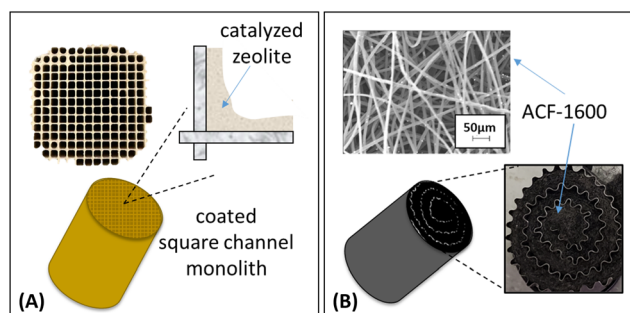

Fig. 1 Schematic showing the general structure of the adsorbents studied: (A) zeolite-based adsorbent washcoated on an open channel monolith and (B) ACF-1600 felt adsorbent rolled between corrugated metal.
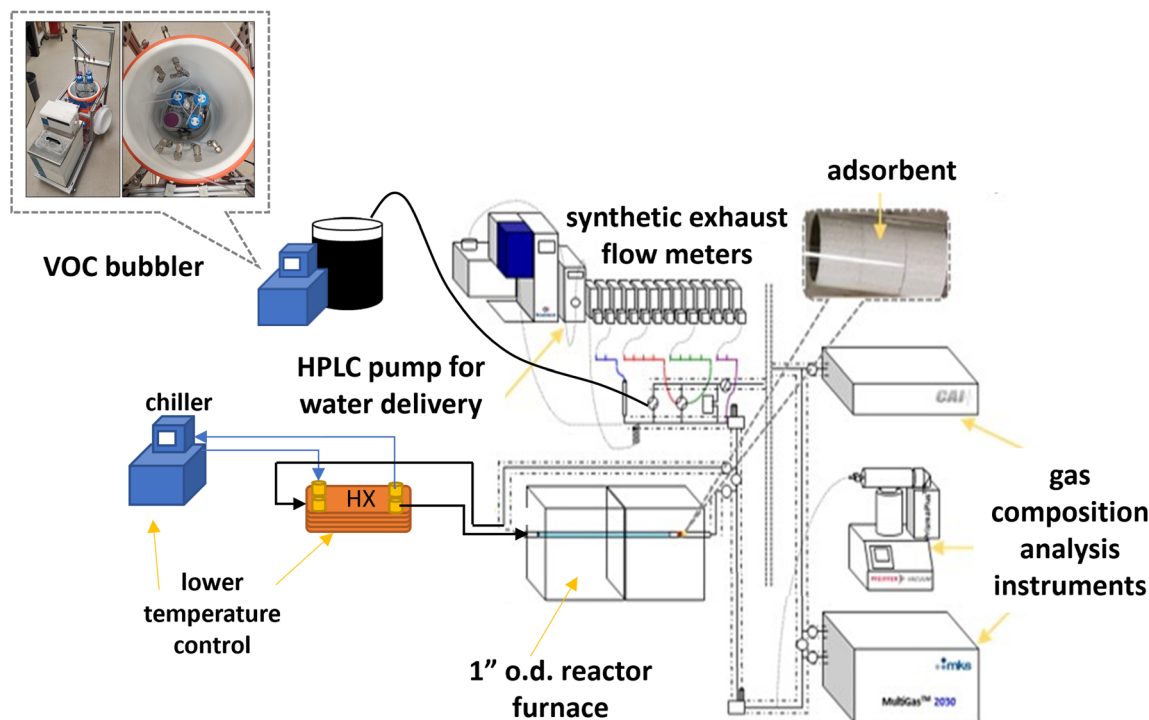
Fig. 2   Schematic of bench reactor layout used for measuring adsorbent's toluene adsorption and desorption behavior from a contaminated air flow.

rates in volumetric units at standard conditions (0 °C, 100 kPa). A custom bubbler system was used to introduce toluene to the air flow by bubbling a portion of the nitrogen through liquid toluene at 10 °C; the toluene bubbler bottles were suspended in a circulating water bath. A custom vaporization system was used to introduce water vapor into a heated nitrogen flow using a high-pressure liquid chromatography (HPLC) pump (Eldex Optos 1MP) before mixing with the other synthetic air components. All reactor experiments used a nominal, 30 °C, 42% RH air flow at 7.2 standard liters per minute (slpm or L min^{-1}). The actual relative humidity was calculated based on the concentration of water measured by a downstream Fourier Transform infrared spectrometer (FTIR) and the temperature of the synthetic air at the inlet of the adsorbent. To achieve low-temperature measurements, despite the warm laboratory temperatures and gas heating from water vapor introduction, the toluene-doped and humidified synthetic air feed was passed through a cooled heat exchanger (HX) to lower the mixed-gas temperature to laboratory temperatures. It was important not to drop the heat exchanger below the dew point of either water or toluene. A quartz tube (22 mm ID × 25 mm OD × 0.97 m long) was used to position the adsorbents at the center of a tube furnace (Lindberg/Blue M™ Mini-Mite™). The zeolite-based adsorbent on a cordierite monolith (Fig. 1(A)) was cut to fit inside the quartz tube with a nominal size of 19.7 mm OD × 77.1 mm length (157 channels; 19.53 cm^3). The ACF-1600 was cut to size and measured and weighed (0.9885 g; 1483 mm^2) before "jelly rolling" it inside a thin wavy steel sheet to create the cylindrical sample as shown in Fig. 1(B), with a nominal size

of 19.7 mm OD × 43.8 mm length. Both adsorbents were wrapped with high-temperature alumina oxide ceramic fiber (Cotronics Corp.) to create a tight seal against the walls of the tube to eliminate gas bypassing the adsorbent samples. The face velocity, which was calculated by dividing the air flow rate by the cross-sectional area of the adsorbent, was 0.4 m s^{-1}. Due to the design of this test system, temperatures discussed will represent inlet gas temperatures. While many adsorption studies focus on only heating the adsorbent, the future application considered here is in a HVAC system to allow in-line regeneration. In this type of application, the heated gas during regeneration would be vented outside the building with the removed VOC.

Toluene concentrations were measured with a MKS MultiGas 2020, 5 Hz fast-response FTIR using the "Aromatic as C7" measurement from a MKS calibrated analysis method. All FTIR data was measured at a 1 s resolution. To dampen measurement noise at low FTIR concentration readings, the 1 s sampling measurements were smoothed using a 15 s running average for final graphing of the toluene breakthrough data; all prior data processing was done directly to the 1 s sampling measurements. The gas-feed toluene concentration was controlled by adjusting the fractional N_2 flow to the toluene bubbler and confirmed by bypassing measurements prior to evaluation. Once the target feed toluene concentration was confirmed, the gas flow was routed through the quartz tube allowing the toluene concentration downstream of the adsorbent to be continuously measured. The toluene in the synthetic air feed could be switched on and off using a heated 4-way switching valve which

sent the equivalent N_2 flow to the gas mixture when toluene-free air feed was required.

Adsorption studies were performed for each adsorbent at 30 °C using different toluene concentrations in the feed air flow; the specific toluene concentration used for a given measurement is referred to as the "challenge" concentration. Breakthrough curves use the upstream (feed) and downstream (post adsorbent) toluene concentrations to show the fraction of the toluene ($T_{b\%}$) that breaks through the adsorbent (*i.e.* not adsorbed) over the duration of a toluene challenge study according to eqn (3). Where C_{feed} was the toluene challenge concentration measured during sample bypass, while C was the toluene concentration measured downstream of the adsorbent.

$$T_{b\%} = \frac{C_{feed} - C}{C_{feed}} \times 100\% \quad (3)$$

Toluene mass adsorption rates, $\dot{m}_{ads}$, were calculated from FTIR concentrations according to eqn (4). Where MW was the molecular weight of toluene, Q_{tot} was the total gas flow rate and $V_{mol,0°C}$ was the molar volume of gas at STP (0 °C). The toluene mass feed rates, $\dot{m}_{feed}$, were calculated from adsorbent bypass measurements (C_{feed}) taken prior to the challenge study and calculated according to eqn (5).

$$\dot{m}_{ads} = \frac{(C_{feed} - C) \times Q_{tot} \times MW}{V_{mol,0°C}} \quad (4)$$

$$\dot{m}_{feed} = \frac{C_{feed} \times Q_{tot} \times MW}{V_{mol,0°C}} \quad (5)$$

Using the FTIR measurements of the downstream toluene concentration, C, allowed the $\dot{m}_{ads}$ to be calculated at a 1 s resolutions. After accounting for this one second interval, a continual summation according to eqn (6), where $\dot{m}$ is $\dot{m}_{ads}$ from eqn (4), provides the toluene mass adsorption data as a cumulative adsorption, Δm_{ads}.

$$\Delta m_t = \sum_{t=0}^{t} \dot{m} \Delta t \quad (6)$$

Since the toluene C_{feed} will influence cumulative adsorption as a function of time and this study investigated different C_{feed}, the cumulative toluene mass adsorption will be plotted as a function of the corresponding cumulative toluene mass feed, Δm_{feed}, to enable direct comparisons between the different challenge concentration tests. The Δm_{feed}, was calculated using eqn (5) and (6) where $\dot{m}$ in eqn (6) is $\dot{m}_{feed}$ from eqn (5).

Prior to each of the three repeated adsorption cycles, the adsorbent was pretreated in the clean synthetic air flow described above (including H_2O, CO_2, O_2 and N_2) at 300 °C for 10 min and then cooled to the adsorption challenge test temperature all in the absence of toluene. Following each adsorption challenge study, the toluene dopant was removed from the synthetic air feed while the air flow continued passing through the adsorbent for 5 min before preparing the reactor for a desorption step to regenerate the adsorbent for a repeated adsorption cycle and provided information about reversible

toluene adsorption at the 30 °C adsorption temperature. To prepare the sample for the next toluene challenge concentration measurement, the tube furnaces were ramped from 30 °C to 300 °C at 5 °C min⁻¹ to heat the inlet air and adsorbent sample to release the adsorbed toluene under a process known as temperature program desorption (TPD). The toluene desorption rates were measured by the FTIR and converted to mass desorption rates ($\dot{m}_{de}$) and cumulative mass desorbed ($\Delta \dot{m}_{de}$) according to eqn (6) and (7) directly from the downstream toluene concentrations measured after toluene was removed from the feed and during the TPD, where $\dot{m}$ in eqn (6) is $\dot{m}_{de}$ from eqn (7).

$$\dot{m}_{de} = \frac{C \times Q_{tot} \times MW}{V_{mol,0°C}} \quad (7)$$

Each adsorbent sample was tested over three cycles of adsorption and desorption. The TPD enabled reproducible evaluation of the adsorbent's toluene adsorption performance, and all adsorption results are presented as averages across the three adsorption cycles, with error bars indicating the minimum/maximum values.

In addition to enabling repeated adsorption cycles, the TPD studies were used to investigate the regeneration potential of the adsorbents to extend their in-use application and useful life. Since reproducible TPD results had already been established during our pilot studies for these adsorbents, the impact of the oxidative environment on adsorbent regeneration was studied up to 300 °C using a different environment after each of the three adsorption cycles. For each toluene challenge concentration, the cycle 1 TPD was run in an inert N_2 only feed, the cycle 2 TPD was run in a dry air feed containing 20% O_2; the cycle 3 TPD contained the same humidified air feed used for all the adsorption cycles (42% RH at 30 °C). A full humidified air feed was introduced at 300 °C for 10 min after all TPD ramp cycles to ensure complete removal of toluene.

3. Results and discussion

3.1. Maximum adsorption capacity

Fig. 3 shows the adsorption isotherms of toluene for the zeolite- and ACF-based adsorbents in dry air at different toluene partial pressures (P/P_0). The maximum adsorption capacities can be obtained from the isotherm curve. The dry toluene adsorption on a small 30-channel sample of the zeolite-based adsorbent was repeated three times. The averaged adsorption isotherm results normalized by M_{ZB} in Fig. 3(A) showed a type II isotherm,[27,28] indicating multilayer adsorption. An adsorption capacity of 117 mg g⁻¹ was achieved at 10% P/P_0. Further increase in the toluene partial pressure led to an exponential increase in the adsorption capacity due to the multilayer adsorption in the mesopores or macropores. The maximum adsorption capacity ($\Delta m_{cap,max}$) reached 263 mg g⁻¹ at 90% P/P_0 under these dry air conditions.

The average dry toluene adsorption for three ACF adsorbent samples, normalized by M_{ACF}, is shown in Fig. 3(B). The adsorption of toluene on ACF-1600 exhibits Type I isotherm,[27,28]

454 | *Environ. Sci.: Adv.*, 2026, **5**, 450–462

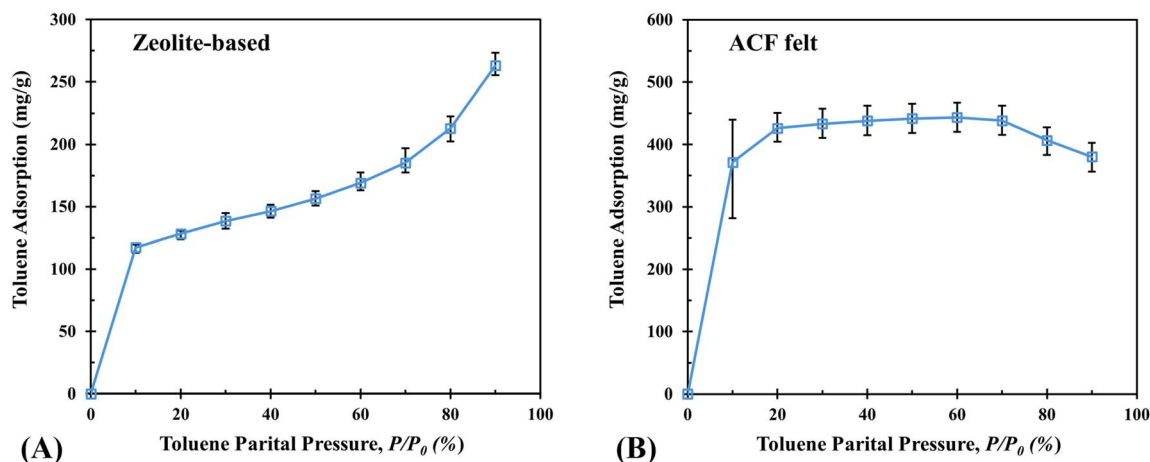© 2026 The Author(s). Published by the Royal Society of Chemistry

Fig. 3 Adsorption isotherm of toluene (dry) on zeolite-based (A) and ACF-1600 (B) adsorbents. The capacity was normalized by absorbent mass. Error bars indicate the min and max range of the data.

where a significant onset absorption capacity of 372 mg g^{-1} was observed at 10% P/P_0. The substantial onset-adsorption at low P/P_0 implies that toluene molecules can be adsorbed through micropore filling despite the lower partial pressure.[29] Further increasing of the toluene P/P_0 provided little increase in adsorbed capacity, which maxed out at 444 mg g^{-1} at 60% P/P_0 ($\Delta m_{cap,max}$). The toluene adsorption capacity dropped beyond that peak toluene partial pressure suggesting toluene desorption from the ACF adsorbent. As can be seen by error bars in Fig. 3(B), this phenomenon was repeatedly observed for all three toluene challenge studies. Toluene can be adsorbed on the carbon material through different potential interactions, including (1) hydrophobic effect, (2) π–π interaction, (3) hydrogen bonds, (4) van der Waals force, and (5) covalent and electrostatic interactions.[10] Toluene–toluene interactions are around 11 kJ mol^{-1}.[30] Physical adsorption mechanisms like van der Waals forces and hydrophobic binding forces are relatively weak, and usually on the order of 10 kJ mol^{-1} and 5 kJ mol^{-1},[30] respectively. When toluene P/P_0 is high, the toluene adsorbed through such weak interactions could desorb due to the stronger toluene–toluene interactions. This could be the origin of the decreasing toluene adsorption observed in Fig. 3(B) at high P/P_0. At 90% P/P_0 of toluene the adsorption capacity dropped to 380 mg g^{-1} under these dry air conditions.

3.2. Zeolite-based adsorbent

3.2.1. Toluene breakthrough. The adsorption capacity of the zeolite-based adsorbent in synthetic air at 30 °C and 42% RH was studied on the bench flow reactor. Since IAQ applications occur in humidified air and as both adsorbents can also adsorb ambient water vapor, the adsorption capacities derived from these studies will be considered the adsorbent's effective adsorption capacity (Δm_{eff}) at this temperature/humidity condition. The results of these studies were evaluated and graphed in two different ways: (1) as time-based breakthrough curves and (2) cumulative mass based adsorption efficiency. These breakthrough curves show the fraction of the upstream

feed toluene measured downstream of the adsorbent ($T_{b\%}$) at a given time, according to eqn (3), indicating how much toluene was not adsorbed at a given time and is a great way to compare the efficiency of different adsorbents under the same conditions. Since the $T_{b\%}$ is specific to a point in time, it will be dependent on how much toluene was in the challenge feed and how much of the adsorbate had been previously adsorbed. Therefore, to compare an adsorbent's adsorption efficiency in relation to its total (i.e. cumulative) effective adsorption capacity at different challenge concentrations the data was also plotted as the cumulative mass of toluene adsorbed as a function of the cumulative mass to which it had been exposed.

Fig. 4(A) shows the breakthrough times ($t_{b\%}$) for the zeolite-based adsorbent challenged at three different toluene concentrations (60, 140 and 200 ppm). The 60 ppm study resulted in almost no breakthrough, with an average of 1% breakthrough after 30 minutes and 4% after 70 minutes for three repeated cycles. After 60 minutes in the 200 ppm study, nearly 100% breakthrough occurred and continued for the remainder of the adsorption cycle. The 140 ppm study showed $T_{5\%}$ halfway through the toluene adsorption cycle and just over $T_{50\%}$ at its completion. Breakthrough time for $T_{5\%}$ of the 200 ppm toluene challenge took 26 minutes and twice that time to reach $T_{50\%}$. An additional 14 minutes were needed to reach $T_{95\%}$ at 64 minutes. The non-linear adsorption rate of toluene suggests that there may be more than one type of adsorption site with different toluene affinities. Table 1 reports the average breakthrough times ($t_{b\%}$) measured at 5%, 50% and 95% toluene breakthrough and the corresponding cumulative mass of toluene that had been challenged ($\Delta m_{feed,b\%}$) at the time of breakthrough ($\Delta m_{b\%}$) according to eqn (8), where the toluene mass feed rate ($\dot{m}_{feed}$) was calculated from eqn (5) and $t_{b\%}$ measured can be found in Table 1. While the breakthrough times are different for different toluene challenge concentrations, the cumulative masses of toluene that had been challenged are very close.

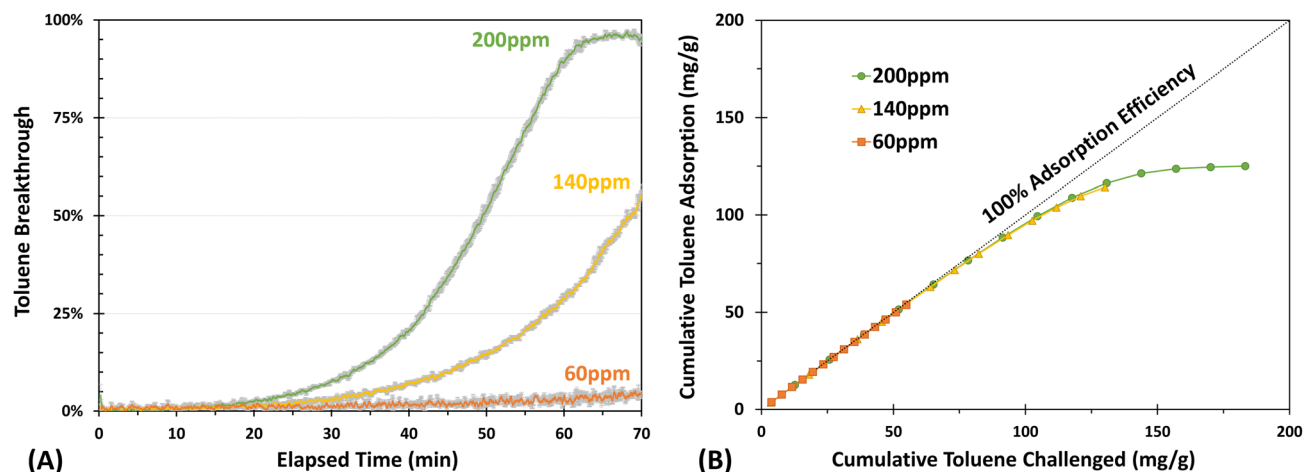$$\Delta m_{feed,b\%} = \dot{m}_{feed} \times t_{b\%} \tag{8}$$

Fig. 4 (A) Average toluene challenge breakthrough results for the zeolite-based adsorbent over 70 min at three different toluene concentrations: 200 ppm (green), 140 ppm (yellow), 60 ppm (orange). Gray error bars indicate min and max of three cycles. (B) Corresponding average cumulative toluene adsorbed per unit mass of washcoated adsorbent for all three challenge concentrations as a function of cumulative toluene challenged (*i.e.* exposed), every 5 min. The curves and points are the average of the results from three adsorption–desorption cycles. 100% adsorption reference is indicated by dotted line (black).

Table 1 Zeolite-based adsorbent's toluene breakthrough times and corresponding mass challenged

	Toluene challenge $t_{b\%}$ $(\Delta m_{\text{feed},b\%})^a$		
	60 ppm	140 ppm	200 ppm
$T_{b5\%}$	—	35 min (65 mg g^{-1})	26 min (68 mg g^{-1})
$T_{b50\%}$	—	69 min (126 mg g^{-1})	50 min (130 mg g^{-1})
$T_{b95\%}$	—	—	64 min (167 mg g^{-1})

^{a} 3 cycle average of toluene breakthrough mass/mass adsorbent are for sample configuration of this study with 30 °C, 42% RH air at 7.2 lpm.

When the average toluene cumulative adsorption was correlated to the mass of toluene challenged, as shown in Fig. 4(B), the results of the three challenge concentrations collapsed to a single adsorption efficiency curve. While cumulative mass adsorption was derived at every second of the transient adsorption data, to aide in visual comparison between the different challenge concentrations in the Fig. 4(B) graph only the cumulative adsorption every 5 min is represented with markers in the plots. The strong correlation of mass adsorptions across the toluene concentrations indicated that the effective adsorption capacity for the zeolite-based adsorbent was not dependent on the VOC partial pressure, which notably differs from the adsorption isotherm study using percent challenge levels shown in Fig. 3. A 100% cumulative toluene removal efficiency was maintained, on the sample studied, up to 84 mg g^{-1} (±2 mg g^{-1}, 2.5%) of cumulative toluene exposure. Once the toluene challenge exceeded 84 mg g^{-1}, the removal efficiency began to drop until the adsorbent reached saturation. Since the 200 ppm study was the only concentration studied to reach saturation within challenge times studied, it was used to derive the average toluene saturation adsorption capacity of 125 mg g^{-1}.

The zeolite-based adsorbent was exposed to 55 mg g^{-1} toluene cumulatively over the 60 ppm challenge study which resulted in only 4% breakthrough of the toluene contaminant (Fig. 4(A)) and negligible deviation from the 100% cumulative removal efficiency reference line (Fig. 4(B)) by the end of the study. In the 140 ppm and 200 ppm challenge studies, which were exposed to 130 and 184 mg g^{-1} cumulative toluene, respectively, a significant drop (>2.5%) in the removal efficiency began in both studies after it exceeded 84 mg g^{-1}, as highlighted by the deviation from the 100% adsorption efficiency reference line in Fig. 4(B).

At the end of each adsorption cycle, toluene was removed from the synthetic air feed while the humidified air flow continued for at least 5 min. Reversible toluene desorption from the zeolite-based adsorbent at 30 °C adsorption temperature occurred in both the 140 ppm and 200 ppm challenge studies without heating, but not in the 60 ppm study. The occurrence of reversible toluene desorption (*i.e.* out-gassed) was only observed in studies that resulted in a significant drop from 100% cumulative removal efficiency suggests the presence of more than one type of adsorption site in the zeolite-based adsorbent studied. Since nothing was desorbed in the 60 ppm study, it suggested that the adsorbed toluene first adsorbs on the stronger sites before adsorbing on sites prone to passive desorption by 30 °C. The sites that more strongly adsorbed toluene would likely be between the 54 mg g^{-1} adsorbed during the 60 ppm study and the 84 mg g^{-1} adsorbed during the 140 ppm and 200 ppm study before the cumulative toluene removal efficiency dropped below 100%.

While water and toluene can compete for the same adsorption sites in the zeolite-based adsorbents, no roll-up effect on the toluene adsorption was observed in this study. A roll-up effect is typically indicated in an adsorption study when the breakthrough concentration is greater than that in the feed gas

due to competitive adsorption displacing a previously adsorbed species.[31] Water has been reported to more strongly interact with many adsorbents displacing previously adsorbed VOCs to cause this roll-up effect but both adsorbent properties and humidity conditions can have an impact.[32,33] The adsorbents in our study were already exposed to water vapor during pretreatment, cooling and stabilization at 30 °C such that by the time toluene was introduced to the feed gas adsorptions sites which favored water would have already been saturated. The lower humidity and length of the adsorption tests in this study may have also contributed to no roll-up effect being observed.

3.2.2. Toluene desorption. Since each toluene concentration resulted in different total toluene challenge masses and adsorption quantities, Fig. 5 presents the TPD results in terms of the mass of toluene still adsorbed on the zeolite-based adsorbent as a function of temperature. In the studies presented, any toluene adsorbed during an adsorption cycle that had not been measured as toluene after the toluene challenge contaminant was removed from the feed gas was considered as still adsorbed on the adsorbent.

The 60 ppm study resulted in no more than 4% toluene breakthrough resulting in nearly 100% cumulative removal efficiency during the adsorption cycles. Only 1% of the adsorbed toluene passively desorbed between the adsorption and desorption steps in that study suggesting the toluene remained securely adsorbed in the zeolite-based adsorbent until the TPD temperature rose above 70 °C in any of the feed gas environments, see orange plots in Fig. 5. In the inert and dry oxidizing environments of TPD 1 (solid lines) and TPD 2 (dashed lines), greater than 10% desorption of the toluene did not occur until the inlet air reached 90 °C followed by a steady disruption until 150 °C. In the humidified air environment of the TPD 3 (dotted lines), toluene desorption began 10 °C cooler at 80 °C and

resulted in more total toluene desorbed compared to the other dry desorption environments. The competitive adsorption between water and toluene at low temperature is expected to play a role in the lower temperature desorption in humidified air. While the zeolite-based adsorbent was designed for enhanced hydrocarbon trapping near ambient temperature, water adsorption will be stronger than the toluene on many of the zeolite adsorption sites, such as the hydrophilic Brønsted acid sites. This weakening of the toluene adsorption may contribute to the lower temperature required for it to desorb in the presence of water. This is in line with water's strong competitive adsorption with toluene on zeolites.[18,34]

While the 200 ppm study exposed the zeolite-based adsorbent to 54 mg g^{-1}, more toluene than the 140 ppm study, it only resulted in a slight increase in the maximum effective adsorption from 117 to 125 mg g^{-1}, respectively. However, the 200 ppm and 140 ppm studies only maintained 100 mg g^{-1} ($\pm$5 mg g^{-1}) adsorbed by the start of the TPDs. The reduction in adsorbed toluene from the maximum effective adsorption capacity indicated passive toluene desorption. This passive desorption can be seen in Fig. 5 from the drop in mass from the maximum effective adsorption capacities (symbols) and the mass remaining on the adsorbent at the start of the TPDs (line plots). In the humidified air environment of TPD 3 (dotted plots), the two higher toluene challenge studies followed similar temperature desorption profiles until about 120 °C. Therefore, under the humified air adsorption conditions of these studies, the zeolite-based adsorbent used could adsorb up to 125 mg g^{-1} of toluene but at least 25 mg g^{-1} would readily desorb in the absence of a toluene contaminant at 30 °C indicating at least 25 mg g^{-1} of reversible toluene adsorption capacity. Considering the drop from 100% adsorption efficiency in Fig. 4(B) occurred at 84 mg g^{-1} cumulative adsorption, it is probable that over an extended time at 30 °C the net reversible capacity may have increased up to 41 mg g^{-1} as the capacity dropped to 84 mg g^{-1} until exposure to higher temperatures. Since the toluene adsorption was consistent for the three repeated adsorption cycles, the differences in the amount of toluene remaining at the end of each TPD cycle in Fig. 5 may be due to toluene conversion during the TPD rather than toluene still adsorbed. Further studies are ongoing to better understand the regeneration approach, including if any conversion products are generated and correlation with the TPD environment.

3.3. ACF-1600 adsorbent

3.3.1. Toluene breakthrough. Toluene breakthrough times on the ACF adsorbent are shown in Fig. 6(A) under three toluene challenge concentrations (60, 140, and 200 ppm). Since complete saturation of the ACF was not achieved within 70 min, the 140 ppm study time was extended to determine the effective adsorption capacity. The adsorbent breakthrough results were reproducible across the three adsorption cycles run for each toluene challenge concentrations. Correlation of the toluene mass breakthrough with the mass of toluene challenged, see Fig. 6(B), shows that the adsorption results are the same for all three challenge concentration studies. Under the ACF sample
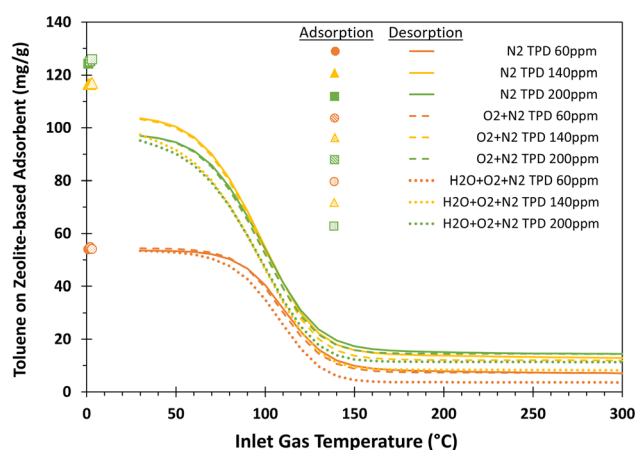

Fig. 5 TPD results plotted as toluene remaining on the zeolite-based adsorbent per unit mass of the washcoated adsorbent as function of temperature. Legend indicates TPD environment [N$_2$ (solid), O$_2$ + N$_2$ (dashed) or H$_2$O + O$_2$ + N$_2$ (dotted)] and toluene concentration used in preceding adsorption cycle [60 ppm (orange, ○), 140 ppm (yellow, △) or 200 ppm (green, □)]. Symbols indicate the maximum effective adsorption capacity measured during the adsorption cycle and are not a function of the temperature.
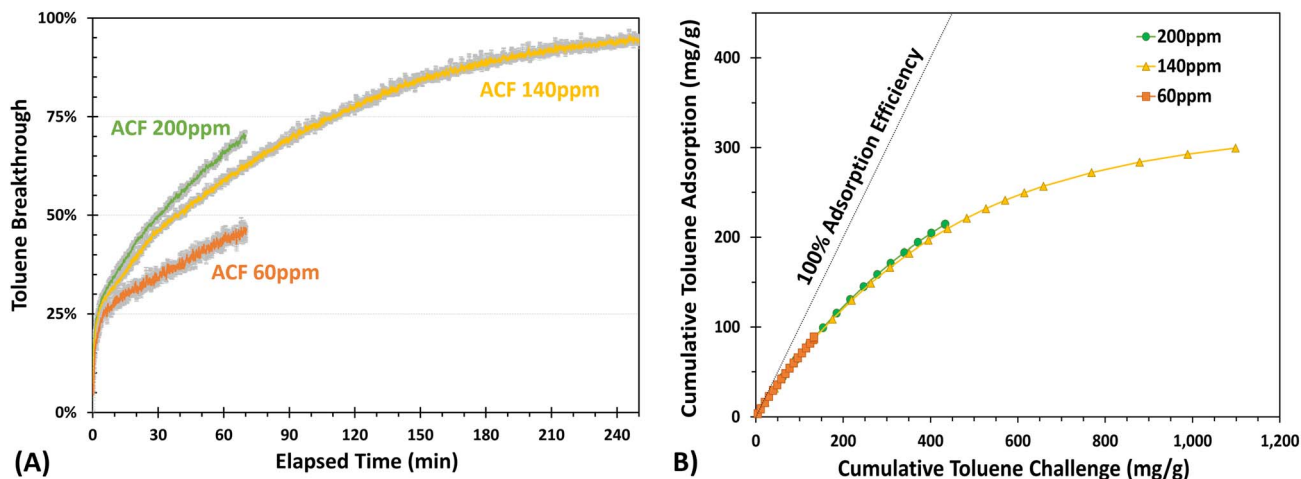
© 2026 The Author(s). Published by the Royal Society of Chemistry

Environ. Sci.: Adv., 2026, **5**, 450–462 | **457**

Fig. 6 (A) Average toluene challenge breakthrough results for the ACF-1600 adsorbent at three different toluene concentrations: 200 ppm (green), 140 ppm (yellow), 60 ppm (orange). Gray error bars indicate min and max of three cycles. (B) Corresponding average cumulative toluene adsorbed per unit mass of ACF for all three challenge concentrations as a function of cumulative toluene challenged (*i.e.* exposed). For simplicity, only data every 10 min was plotted up to 150 min, thereafter only every 25 min. Dotted line (black) indicates what would have been 100% adsorption efficiency.

Table 2 ACF adsorbent's toluene breakthrough times and corresponding mass challenged

	Toluene challenge $t_{b\%}$ ($\Delta m_{\text{feed},b\%}$)[a]		
	60 ppm	140 ppm	200 ppm
$T_{b5\%}$	0.4 min (0.8 mg g^{-1})	0.1 min (0.5 mg g^{-1})	0.1 min (0.7 mg g^{-1})
$T_{b50\%}$	—	38 min (167 mg g^{-1})	30 min (190 mg g^{-1})
$T_{b95\%}$	—	248 min (1102 mg g^{-1})	—

[a] Toluene breakthrough masses are for sample configuration of this study with 30 °C, 42% RH air at 7.2 lpm.

configuration studied, 25% or higher toluene breakthrough was consistently observed. Further studies are required to determine if a different ACF adsorbent design configuration would lower the toluene breakthrough at the start of exposure. While 100% adsorption efficiency was not seen for the ACF adsorbent, the rate of breakthrough slowed after the toluene mass challenged exceeded 202 mg g^{-1}. In the 140 ppm study, the ACF had just reached $T_{95\%}$ toluene breakthrough at the end of the 250 min adsorption study, indicating a toluene maximum effective capacity of 296 mg. When the ACF sample studied at a 0.4 m s^{-1} face velocity was normalized by the sample used, the toluene effective adsorption capacity was 300 mg g^{-1} (0.20 mg mm^{-2}). Table 2 reports breakthrough times ($t_{b\%}$) and the corresponding cumulative toluene mass challenged ($\Delta m_{\text{feed},b\%}$) at time of breakthrough according to eqn (8). Similar to the zeolite-based adsorbent, no roll-up effect for toluene was observed on the ACF felt used under these test conditions.

3.3.2 Toluene desorption. Regeneration of the ACF was performed using the same method as the zeolite-based adsorbent investigating the same three TPD environments: (1) inert; (2) dry oxidizing; (3) humidified air. The mass of toluene that remained on the ACF as function of temperature throughout the TPD for each environment and challenge concentration studied is shown in Fig. 7, with the mass of maximum effective

toluene capacity represented by symbols. No trend was seen across the nine different TPD cycles to indicate a strong influence from the TPD environment, suggesting temperature alone was the major driver for desorption from the ACF adsorbent.

The drop in mass from the maximum effective adsorption capacities, attained at the end of the adsorption cycles, (symbols) plotted in Fig. 7 to the mass remaining on the adsorbent at the start of the TPDs (line plots) indicates the passive desorption that occurred on the ACF adsorbent. Even though more than 50% less toluene had been adsorbed on the ACF during the 60 ppm challenge study compared to the 140 ppm and 200 ppm studies, a notable 7–8% of that adsorbed toluene passively desorbed before the start of the desorption step. Unlike the zeolite-based adsorbent, no overlap in the mass remaining on the ACF adsorbent as function of temperature was seen between the different challenge studies. The ACF adsorbent during the 140 ppm challenge study, which resulted in the greatest toluene adsorption due to exposure time, retained notably more adsorbed toluene during the TPD. These desorption results suggest that while higher temperatures may accelerate toluene desorption from the adsorbent, other properties of the ACF are significant contributors to the rate of toluene desorption.
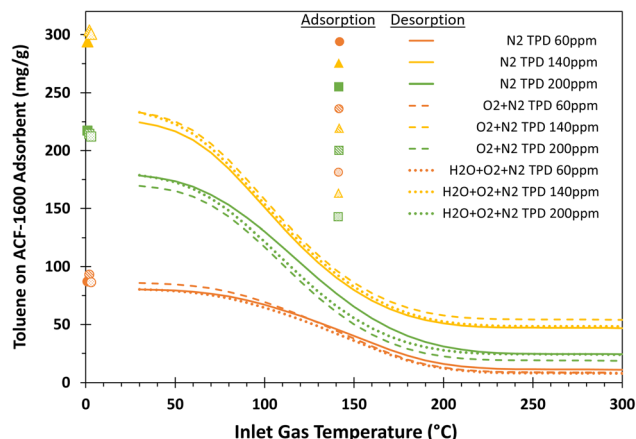
Fig. 7 TPD results plotted as toluene remaining on the ACF-1600 adsorbent per unit ACF mass as a function of temperature. Legend indicates TPD environment [N_2 (solid), O_2 + N_2 (dashed) or H_2O + O_2 + N_2 (dotted)] and toluene concentration used in preceding adsorption cycle [60 ppm (orange, ○), 140 (yellow, Δ) or 200 ppm (green, □)]. Symbols indicate the maximum effective adsorption capacity measured during the adsorption cycle and are not a function of the temperature.

Capacity degradation over the adsorption/regeneration cycles was not observed for either the zeolite-based or ACF felt adsorbent. The same samples were used for the 3 cycle challenge studies for all three toluene challenge concentrations. Fig. 4(A) and 6(A) show the 3 cycle averages with gray error bars to indicate the min and max values of the 3 cycles. The small deviation between the 3 cycles indicated reproducibility of the adsorption capacity for each cycle under the same toluene challenge concentration. Additionally, in Fig. 4(B) and 6(B), the same cumulative adsorption capacity for all three toluene challenge concentrations shows no degradation in the adsorption capacity under three toluene challenge concentrations. Finally, both adsorbents can withstand extended use at significantly higher temperatures than the 300 °C used in this study according to their technical data sheet, so the material structural damage due to the high temperature used in this study was not expected.

3.4. Predicted breakthroughs

While unique for the zeolite and ACF adsorbent samples, the correlation between the amount of toluene exposed and the mass adsorbed was reproducible across a wide range of toluene challenge concentration for both adsorbents. This suggests that for the conditions used in this study, the breakthrough curve data can be used to predict breakthrough times at other toluene concentrations not used in the study. The recommended high and low standard challenge concentrations for toluene according to ANSI/ASHRAE Standard 145.2–2016 (ref. 35) are 400 ppb and 50 ppm, respectively. Table 3 reports the predicted breakthrough times ($t_{b\%}$) at these concentrations for the zeolite-based and ACF adsorbent samples used in this study based on mass adsorption at 5%, 50% and 95% breakthrough determined during adsorption steps in the 200 ppm and 140 ppm

Table 3 Toluene breakthrough time predictions ($t_{b\%,\mathrm{pred}}$) based on toluene challenge study $\Delta m_{\mathrm{feed},b\%}$ for sample configurations and flow rates used in study presented

	400 ppb challenge concentration			50 ppm challenge concentration		
	Toluene $t_{b\%}{}^a$ (days)			Toluene $t_{b\%}{}^a$ (h)		
	$t_{5\%}$	$t_{50\%}$	$t_{95\%}$	$t_{5\%}$	$t_{50\%}$	$t_{95\%}$
Zeolite	9.6	18.1	23.3	1.8	3.5	4.5
ACF	(0.7h)	9.7	63.9	(< 1 min)	1.9	12.3

^{a} Breakthrough times assume 7.2 lpm flow for the same sample size/ configuration presented herein and are specific to adsorbent masses used in this study.

challenge studies, respectively. These predicted breakthrough times ($t_{b\%,\mathrm{pred}}$) were calculated according to eqn (9), where $\Delta m_{\mathrm{feed},b\%}$ can be found in Tables 1 and 2 and the mass rate of the prediction feed ($\dot{m}_{\mathrm{feed},\mathrm{pred}}$) was calculated according eqn (5).

$$\frac{\Delta m_{\mathrm{feed},b\%}}{\dot{m}_{\mathrm{feed},\mathrm{pred}}} = t_{b\%,\mathrm{pred}} \tag{9}$$

These predicted results indicate that at the low 400 ppb challenge concentration, the zeolite-based adsorbent would last more than 9 days before 5% breakthrough and twice that before 50% breakthrough. After 50% breakthrough, the toluene removal efficiency drops more quickly reaching 95% breakthrough 5 days later or after 23.3 days of 400 ppb toluene exposure. The ACF breakthrough at 400 ppb shows a different trend reaching 5% breakthrough in less than an hour and 50% in under 10 days. However, 95% breakthrough over the ACF sample would take another 54 days. At the higher 50 ppm challenge concentration, breakthrough for both adsorbents would be measured on the hour scale rather than days but follows a similar trend described for the 400 ppb scenario. The zeolite-based adsorbent provides superior performance for applications requiring low VOC breakthrough. In applications where higher VOC breakthrough is tolerable, the ACF adsorbent can offer longer application times between regeneration events. Further validation of the continued adsorption linearity down to lower toluene concentration conditions is still required.

4. Conclusions

Toluene adsorption capacity and breakthrough times were used to relate toluene removal potential across a range of low to high contamination levels using a zeolite-based and an ACF felt adsorbents. Separate desorption studies showed the influence of environmental conditions on adsorbent regeneration. These studies suggested a stable toluene adsorption capacity of 84 mg g^{-1} without passive desorption on the zeolite-based adsorbent. The adsorbent showed regeneration potential *via* thermal desorption temperatures starting between 60 °C to 70 °C depending on the humidification of the regeneration air and a more rapid toluene release rate above 90 °C with no additional

© 2026 The Author(s). Published by the Royal Society of Chemistry

Environ. Sci.: Adv., 2026, **5**, 450–462 | **459**

desorption above 150 °C. The presence of strong adsorption sites on the zeolite-based adsorbent provided usable effective adsorption capacity without passive desorption. Desorption from these sites was directly dependent on temperature, quickly releasing the toluene at relatively low temperature. The combination of its adsorption capacity not susceptible to passive desorption at room temperature along with its temperature dependent desorption opens the potential for multiple use configurations for indoor VOC removal with in-line regeneration.

The ACF felt adsorbent showed passive desorption under all conditions studied. Its desorption rate was found to be more strongly influenced by the mass of toluene on the ACF than the temperature. While increasing the temperature helped to accelerate rate of desorption, time at the higher temperatures was still required. The slow passive desorption at room temperature and only a moderate acceleration in desorption rate at elevated temperatures may limit its potential effectiveness for some types of indoor VOC control.

On-going studies to further our understanding of the adsorbents will help to confirm the adsorption capacity at which the maximum effective toluene adsorption capacity can be trapped on the adsorbents without passive desorption and if further adsorption capacity can be accessed if upstream humidity control is available. Future studies will also focus on how much adsorption can be recovered at lower regeneration temperatures to provide reusable adsorption capacity.

Abbreviations

ch	Monolith channel
cpsi	Channels per square inch
ZB	Zeolite-based monolith adsorbent
ACF	Activated Carbon Fiber felt adsorbent
DVS	Dynamic Vapor Sorption system
p_{wc_m}	Mass density of washcoat on monolith (g mm^{-3})
M_{ZB}	Mass of washcoated zeolite-based adsorbent sample (mg)
N_{ch}	# of channels in monolith sample (ch)
A_{ch}	Monolith cross-sectional channel area of sample (ch/mm^2)
P/P_0	Partial pressure of toluene
M_{ACF}	Mass of ACF sample (mg)
$\Delta m_{cap,max}$	Maximum adsorption capacity on adsorbent (mg toluene/M_{adsorb}), in dry air
M_{DVS}	Mass of adsorbent after toluene adsorption in DVS exotherm experiments
M_{adsorb}	Mass of fresh adsorbent sample (M_{ZB} or M_{ACF})
$T_{b\%}$	Fraction of toluene mass breakthrough
C_{feed}	Toluene challenge concentration in the feed gas (ppm) measured during bypass
C	Toluene concentration measured downstream of the adsorbent (ppm)
Q_{tot}	Total gas feed volumetric flow rate
MW	Molecular weight of toluene
$V_{mol,0°C}$	Molar volume gas at STP (0 °C)
$\dot{m}$	Toluene mass rate
Δm	Cumulative toluene mass
feed	Toluene challenge
ads	Toluene adsorbed
de	Toluene desorbed
$\Delta m_{eff,max}$	Maximum effective adsorption capacity on adsorbent (mg toluene/M_{adsorb}), in humidified study conditions
$t_{b\%}$	Time till breakthrough% ($T_{b\%}$)

Author contributions

MMD: conceptualization, formal analysis, investigation, methodology, project administration, supervision, visualization; writing – original draft, writing – review & editing; MT: formal analysis, visualization, writing – original draft, writing – review & editing; KL: visualization, investigation, writing – original draft, writing – review & editing; KA: investigation, writing – review & editing; WPP: conceptualization, formal analysis, methodology, supervision, writing – review & editing; KN: funding acquisition, writing – review & editing.

Conflicts of interest

The authors have no conflicts to declare.

Data availability

The test conditions and data processing approach supporting the results of the study presented have been described within the article. The raw data sets can be accessed at https://doi.org/10.13139/ORNLNCCS/2569322.

References

1 S. Altomonte, J. Allen, P. M. Bluyssen, G. Brager, L. Heschong, A. Loder, S. Schiavon, J. A. Veitch, L. Wang and P. Wargocki, Ten questions concerning well-being in the built environment, *Build. Environ.*, 2020, **180**, 106949, DOI: 10.1016/j.buildenv.2020.106949.

2 N. E. Klepeis, W. C. Nelson, W. R. Ott, J. P. Robinson, A. M. Tsang, P. Switzer, J. V. Behar, S. C. Hern and W. H. Engelmann, The National Human Activity Pattern Survey (NHAPS): a resource for assessing exposure to

460 | *Environ. Sci.: Adv.*, 2026, **5**, 450–462

© 2026 The Author(s). Published by the Royal Society of Chemistry

environmental pollutants, *J. Exposure Sci. Environ. Epidemiol.*, 2001, **11**(3), 231–252, DOI: 10.1038/sj.jea.7500165.

3 A. H. Goldstein, W. W. Nazaroff, C. J. Weschler and J. Williams, How Do Indoor Environments Affect Air Pollution Exposure?, *Environ. Sci. Technol.*, 2021, **55**(1), 100–108, DOI: 10.1021/acs.est.0c05727.

4 Y. Huangfu, N. M. Lima, P. T. O'Keeffe, W. M. Kirk, B. K. Lamb, V. P. Walden and B. T. Jobson, Whole-House Emission Rates and Loss Coefficients of Formaldehyde and Other Volatile Organic Compounds as a Function of the Air Change Rate, *Environ. Sci. Technol.*, 2020, **54**(4), 2143–2151, DOI: 10.1021/acs.est.9b05594.

5 L. Zhong, F.-C. Su and S. Batterman, Volatile Organic Compounds (VOCs) in Conventional and High Performance School Buildings in the U.S, *Int. J. Environ. Res. Public Health*, 2017, **14**(1), 100, DOI: 10.3390/ijerph14010100.

6 J. M. Logue, T. E. McKone, M. H. Sherman and B. C. Singer, Hazard assessment of chemical air contaminants measured in residences, *Indoor Air*, 2011, **21**(2), 92–109, DOI: 10.1111/j.1600-0668.2010.00683.x.

7 X. Wu, M. G. Apte, R. Maddalena and D. H. Bennett, Volatile organic compounds in small- and medium-sized commercial buildings in California, *Environ. Sci. Technol.*, 2011, **45**(20), 9075–9083, DOI: 10.1021/es202132u.

8 M. A. Sidheswaran, H. Destaillats, D. P. Sullivan, S. Cohn and W. J. Fisk, Energy efficient indoor VOC air cleaning with activated carbon fiber (ACF) filters, *Build. Environ.*, 2012, **47**, 357–367, DOI: 10.1016/j.buildenv.2011.07.002.

9 ASHRAE, *ANSI/ASHRAE Standard 62.1 – Ventilation and Acceptable Indoor Air Quality*, 2022.

10 X. Zhang, B. Gao, A. E. Creamer, C. Cao and Y. Li, Adsorption of VOCs onto engineered carbon materials: A review, *J. Hazard. Mater.*, 2017, **338**, 102–123, DOI: 10.1016/j.jhazmat.2017.05.013.

11 X. Wang, H. Cheng, G. Ye, J. Fan, F. Yao, Y. Wang, Y. Jiao, W. Zhu, H. Huang and D. Ye, Key factors and primary modification methods of activated carbon and their application in adsorption of carbon-based gases: A review, *Chemosphere*, 2022, **287**, 131995, DOI: 10.1016/j.chemosphere.2021.131995.

12 J. Gonzalez-Martín, N. J. R. Kraakman, C. Perez, R. Lebrero and R. Munoz, A state-of-the-art review on indoor air pollution and strategies for indoor air pollution control, *Chemosphere*, 2021, **262**, 128376, DOI: 10.1016/j.chemosphere.2020.128376.

13 A. Bastani, C.-S. Lee, F. Haghighat, C. Flaherty and N. Lakdawala, Assessing the performance of air cleaning devices – a full-scale test method, *Build. Environ.*, 2010, **45**(1), 143–149, DOI: 10.1016/j.buildenv.2009.05.008.

14 N. Mohan, G. K. Kannan, S. Upendra, R. Subha and N. S. Kumar, Breakthrough of toluene vapours in granular activated carbon filled packed bed reactor, *J. Hazard. Mater.*, 2009, **168**(2–3), 777–781, DOI: 10.1016/j.jhazmat.2009.02.079.

15 D. Das, V. Gaur and N. Verma, Removal of volatile organic compound by activated carbon fiber, *Carbon*, 2004, **42**(14), 2949–2962, DOI: 10.1016/j.carbon.2004.07.008.

16 Q. Ye, Y. Chen, Y. Li, R. Jin, Q. Geng and S. Chen, Management of typical VOCs in air with adsorbents: status and challenges, *Dalton Trans.*, 2023, **52**(35), 12169–12184, DOI: 10.1039/D3DT01930F.

17 K.-J. Kim and H.-G. Ahn, The effect of pore structure of zeolite on the adsorption of VOCs and their desorption properties by microwave heating, *Microporous Mesoporous Mater.*, 2012, **152**, 78–83, DOI: 10.1016/j.micromeso.2011.11.051.

18 S. Lu, Q. Liu, R. Han, J. Shi, M. Guo, C. Song, N. Ji, X. Lu and D. Ma, Core–shell structured Y zeolite/hydrophobic organic polymer with improved toluene adsorption capacity under dry and wet conditions, *Chem. Eng. J.*, 2021, **409**, 128194, DOI: 10.1016/j.cej.2020.128194.

19 S. Giraudet, B. Boulinguiez and P. Le Cloirec, Adsorption and Electrothermal Desorption of Volatile Organic Compounds and Siloxanes onto an Activated Carbon Fiber Cloth for Biogas Purification, *Energy Fuels*, 2014, **28**(6), 3924–3932, DOI: 10.1021/ef500600b.

20 K. Kosuge, S. Kubo, N. Kikukawa and M. Takemori, Effect of pore structure in mesoporous silicas on VOC dynamic adsorption/desorption performance, *Langmuir*, 2007, **23**(6), 3095–3102, DOI: 10.1021/la062616t.

21 R. Zhang, Z. Li, X. Wang, F. Wang, L. Zeng and Z. Li, Adsorption equilibrium of activated carbon amid fluctuating benzene concentration in indoor environments, *Build. Environ.*, 2023, **245**, 110964, DOI: 10.1016/j.buildenv.2023.110964.

22 F. Haghighat, C.-S. Lee, B. Pant, G. Bolourani, N. Lakdawala and A. Bastani, Evaluation of various activated carbons for air cleaning – Towards design of immune and sustainable buildings, *Atmos. Environ.*, 2008, **42**(35), 8176–8184, DOI: 10.1016/j.atmosenv.2008.07.061.

23 R. Ligotski, K.-D. Gilles, M. Roehnert, U. Sager, C. Asbach and F. Schmidt, In-situ-desorption of indoor relevant VOC toluene and limonene on activated carbon based filter media using high relative humidity, *Build. Environ.*, 2021, **191**, 107556, DOI: 10.1016/j.buildenv.2020.107556.

24 S. Schumacher, A. Caspari, U. Schneiderwind, K. Staack, U. Sager and C. Asbach, The Drawback of Optimizing Air Cleaner Filters for the Adsorption of Formaldehyde, *Atmosphere*, 2024, **15**(1), 109, DOI: 10.3390/atmos15010109.

25 Y. Sheng, Q. Dong, Q. Ren and M. Wang, Prediction for the Adsorption of Low-Concentration Toluene by Activated Carbon, *Sustainability*, 2023, **15**(2), 1555, DOI: 10.3390/su15021555.

26 K. G. Rappé, C. DiMaggio, J. A. Pihl, J. R. Theis, S. H. Oh, G. B. Fisher, J. Parks, V. G. Easterling, M. Yang, M. L. Stewart and K. C. Howden, Aftertreatment Protocols for Catalyst Characterization and Performance Evaluation: Low-Temperature Oxidation, Storage, Three-Way, and NH₃-SCR Catalyst Test Protocols, *Emiss. Control Sci. Technol.*, 2019, **5**, 183–214, DOI: 10.1007/s40825-019-00120-7.

© 2026 The Author(s). Published by the Royal Society of Chemistry

Environ. Sci.: Adv., 2026, **5**, 450–462 | **461**

27 S. Lowell, J. E. Shields, M. A. Thomas and M. Thommes, *Characterization of Porous Solids and Powders: Surface Area, Pore Size and Density*, Springer Science & Business Media, New York, 2012.

28 S. Brunauer, L. S. Deming, W. E. Deming and E. Teller, On a theory of the van der Waals adsorption of gases, *J. Am. Chem. Soc.*, 1940, **62**(7), 1723–1732, DOI: 10.1021/ja01864a025.

29 H. Deng, T. Pan, Y. Zhang, L. Wang, Q. Wu, J. Ma, W. Shan and H. He, Adsorptive removal of toluene and dichloromethane from humid exhaust on MFI, BEA and FAU zeolites: An experimental and theoretical study, *Chem. Eng. J.*, 2020, **394**, 124986, DOI: 10.1016/j.cej.2020.124986.

30 S. Wjihi, A. Erto, S. Knani and A. B. Lamine, Investigation of adsorption process of benzene and toluene on activated carbon by means of grand canonical ensemble, *J. Mol. Liq.*, 2017, **238**, 402–410, DOI: 10.1016/j.molliq.2017.04.021.

31 K.-D. Kim, E. J. Park, H. O. Seo, M.-G. Jeong, Y. D. Kim and D. C. Lim, Effect of thin hydrophobic films for toluene adsorption and desorption behavior on activated carbon fiber under dry and humid conditions, *Chem. Eng. J.*, 2012, **200–202**, 133–139, DOI: 10.1016/j.cej.2012.06.044.

32 B. Yu, H. Deng, Y. Lu, T. Pan, W. Shan and H. He, Adsorptive interaction between typical VOCs and various topological zeolites: Mixture effect and mechanism, *J. Environ. Sci.*, 2024, **136**, 626–636, DOI: 10.1016/j.jes.2023.02.015.

33 B. Liu, S. A. Younis and K.-H. Kim, The dynamic competition in adsorption between gaseous benzene and moisture on metal-organic frameworks across their varying concentration levels, *Chem. Eng. J.*, 2021, **421**, 127813, DOI: 10.1016/j.cej.2020.127813.

34 B. S. Bal'zhinimaev, E. A. Paukshtis, A. V. Toktarev, E. V. Kovalyov, M. A. Yaranova, A. E. Smirnov and S. Stompel, Effect of water on toluene adsorption over high silica zeolites, *Microporous Mesoporous Mater.*, 2019, **277**, 70–77, DOI: 10.1016/j.micromeso.2018.10.023.

35 ASHRAE, *ANSI/ASHRAE Standard 145.2 – Laboratory Test Method for Assessing the Performance of Gas-Phase Air-Cleaning Systems: Air-Cleaning Devices*, 2016.